European Review for Medical and Pharmacological Sciences 2020; 24: 1357-1366

# LncRNA XIST inhibits hypoxia-induced cardiomyocyte apoptosis *via* mediating miR-150-5p/Bax in acute myocardial infarction

J. ZHOU, D. LI, B.-P. YANG, W.-J. CUI

Department of Cardiovascular, Gansu Provincial Hospital of TCM, Lanzhou, P.R. China

**Abstract. – OBJECTIVE: Acute myocardial infarction (AMI) contributes to long-term cardiac ischemia induced by hypoxia. Long non-coding RNAs (lncRNAs) affect the development and progression of heart diseases. This study explored the role and mechanism of lncRNA X inactive specific transcript (XIST) in H9c2 cells with hypoxia-induced injury.**

**MATERIALS AND METHODS: Methyl-thiazolyl-tetrazolium (MTT), transwell, and flow cytometry assays were employed to analyze the survival, invasion, migration, and apoptosis of H9c2 cells under different conditions, respectively. Expression of related genes was determined by quantitative Real Time-Polymerase Chain Reaction (qRT-PCR) or Western blot.**

**RESULTS: XIST was over-expressed in H9c2 cells with hypoxia-induced injury, and the silence of XIST alleviated cell injury. Up-regulation of XIST promoted the expression of B-cell lymphoma 2-Associated X (Bax) through competitive binding to miR-150-5p.**

**CONCLUSIONS: XIST protects cardiomyocytes from hypoxia-induced injury by mediating miR-150-5p/Bax axis, suggesting that XIST is an important target for AMI treatment.**

*Key Words:*
LncRNA XIST, MiR-150-5p, Bax, Cardiomyocyte, Apoptosis.

## Introduction

Cardiovascular diseases (CVDs) are diseases with the highest morbidity and mortality in the world, and mortality will rise to 36.6% by 2020[1]. As a common CVD, acute myocardial infarction (AMI) poses a great threat to human health[2]. Coronary atherosclerosis-induced vascular stenosis causes myocardial ischemia and hypoxia, resulting in myocardial injury, eventually leading to AMI, and long-term ischemia may lead to cardiomyocyte death[3,4]. Cardiomyocyte necrosis, apoptosis, and subsequent excessive inflammation are the leading causes of cardiomyocyte injury and loss of function[5,6]. However, the mechanisms of AMI have not been clearly explained, so we performed related tests to improve the condition of AMI patients and to provide references for clinical treatment.

Long chain non-coding RNA (lncRNA, >200 nt[7]) was initially considered as a transcriptional "noise" for its incapability to encode proteins directly[8]. However, Bhan et al[9] and Zhang et al[10] found that lncRNA participates in various biological regulatory processes and plays a vital role in angiogenesis, DNA damage, microRNA (miR) silencing, cell invasion and metastasis, and programmed cell death. Zhuo et al[11] point out that lncRNA small nucleolar host gene 8 (SNHG8) is a key regulator of AMI and Yang et al[12] demonstrate that knocking down lncRNA antisense noncoding RNA in the INK4 locus (ANRIL) alleviates cardiomyocyte apoptosis in AMI by regulating IL-33/ST2. LncRNA X inactive specific transcript (XIST) is located on human Xq13.2 chromosome[13] and is highly expressed in liver cancer, lung cancer, and gastric cancer[14-16]. There is evidence that XIST is also highly expressed in AMI[17], but the further mechanism is unclear.

Competing endogenous RNAs (ceRNAs) are newly proposed to reveal the interactions among RNAs. LncRNA affects miR expression by competitive binding to microRNA response elements (MREs), thus regulating transcription of downstream target genes and participating in biological processes[18]. Therefore, in this study, we explored the relevant mechanism of XIST in AMI by analyzing downstream miRs of XIST.

## Materials and Methods

### Cell Culture

H9c2 cells (mouse embryonic cardiomyocytes; American Type Culture Collection, ATCC, Manassas, VA, USA, catalog number: CRL-1446) were cultured in Dulbecco's Modified Eagle's Me-

*Corresponding Author:* Jian Zhou, MD, e-mail: 842821636@qq.com

dium (DMEM; Gibco, Grand Island, NY, USA, catalog number: 11965092) with penicillin (100 U/mL)/streptomycin (100 μg/mL; Gibco, Grand Island, NY, USA, catalog number: 15140163) and 10% fetal bovine serum (FBS; Gibco, Grand Island, NY, USA, catalog number: 16000044). The cells were subject to incubation at 37°C, 95% air and 5% $CO_2$. When reaching 80% confluence, they were transferred to DMEM (0.5% FBS) for 1-hour starvation. To establish hypoxia models, cells were transferred to a hypoxia incubator with 94%$N_2$, 1%$O_2$, and 5% $CO_2$ for 4 h.

### Cell Transfection

The short hairpin RNA (sh-XIST) and the negative control (sh-NC) were designed (GenePharma, Shanghai, China). In addition, pcDNA3.1-Bax (B-cell lymphoma 2-Associated X) was synthesized with Bax sequence and pcDNA3.1(Invitrogen, Carlsbad, CA, USA). Constructed miR-150-5p-mimics and miR-150-5p-inhibit were transfected into H9c2 cells using Lipofectamine 2000 kit (Invitrogen, Carlsbad, CA, USA, catalog number: 11668019) in G418 medium.

### RNA Extraction and Quantitative Real-Time Polymerase Chain Reaction (qRT-PCR)

The total RNAs were sampled with a TRIzol kit (Invitrogen, Carlsbad, CA, USA, catalog number: 15596018), and the purity, concentration, and integrity were measured by an ultraviolet spectrophotometer and agarose gel electrophoresis. Reverse transcription was performed using a TaqMan™ reverse transcription kit (Invitrogen, Carlsbad, CA, USA, catalog number: 4304134). The cDNAs obtained were subjected to subsequent research. PCR amplification was carried out using a PrimeScript RT Master Mix kit (TaKaRa Bio, Otsu, Shiga, Japan, catalog number: RR036B), with the amplification system containing 2 μL cDNA, 0.8 μL each upstream and downstream primers, 10 μL SYBR qPCR Mix, 0.4 μL 50× Rox reference dye, and finally made up to 20 μL with RNase-free water. PCR conditions: pre-denaturation at 95°C for 60 s, denaturation at 95°C for 30 s, annealing, and extension at 60°C for 40 s, for 40 cycles. Three parallel repeating wells were designed, and all samples were repeatedly tested for 3 times. U6 and glyceraldehyde-3-phosphate dehydrogenase (GADPH) were served as internal references, and $2^{-\Delta\Delta ct}$ was used for data analysis[19]. The PCR instrument was 7500PCR from Applied Biosystems (Foster City, CA, USA). The sequence of primers is shown in Table I.

### Cell Viability Assay

After hypoxia induction for 4 h, the cells were transferred to a 96-well plate ($1*10^5$ cells/well) and incubated for 72 h at a 37°C-incubator containing 95% air and 5% $CO_2$. Then, 20 μL methyl thiazolyl tetrazolium (MTT) reagent (5 mg/mL, Invitrogen, Carlsbad, CA, USA, catalog number: M6494) was put into each well, and the supernatant was removed after incubation at 37°C for 4 h. Afterwards, 150 μL dimethyl sulphoxide (DMSO, Invitrogen, Carlsbad, CA, USA, catalog number: D12345) was transferred to each well and shaken for 10 min to ensure full dissolution. A microplate reader was applied to read the optical density (OD) value at 490 nm wavelength.

### Cell Invasion Assay

Cell invasion was determined by transwell. The transfected cells plated in a 6-well plate were incubated for 24 h. The apical chamber was filled with Matrigel (1:20, Corning, Corning, NY, USA) and cells ($1*10^5$ cells/mL) collected using serum-free medium. A total of 750 μL 10% FBS was put into the basolateral chamber. Afterwards, the plate was placed in a 37°C, 5% $CO_2$ incubator for 12 h. The infiltrated cells were permeated for 20 min with methanol and dyed with 0.1% crystal violet in a darkroom. Finally, the cells were quantified using a microscope.

### Cell Apoptosis Assay

Annexin V apoptosis detection kit was employed to determine cell apoptosis. Transfected cells were dyed for 25 min with Annexin V-flu-

**Table I.** Primer sequences.

| Gene | Forward primer | Reverse primer |
|---|---|---|
| LncRNA XIST | 5'-CTCTCCATTGGGTTCAC-3' | 5'-GCGGCAGGTCTTAAGAGATGAG-3' |
| MiR-150-5p | 5'-TCGGCGTCTCCCAACCCTTGTAC-3' | 5'-GTCGTATCCAGTGCAGGGTCCGAGGT-3' |
| Bax | 5'-CCAGCTCTTTAATGCCCGTT-3' | 5'-CGTCCCAAAGTAGGAGAGGA-3' |
| U6 | 5'-ATTGGAACGATACAGAGAAGATT-3' | 5'-GGAACGCTTCACGAATTTG-3' |
| GADPH | 5'-AGCCACATCGCTCAGACAC-3' | 5'-GCCCAATACGACCAAATCC-3' |

orescein isothiocyanate (FITC) and propidium iodide (PI), then evaluated with a flow cytometry (BD FACSCanto™ II; Franklin Lakes, NJ, USA).

### Dual-Luciferase Reporter Assay

DNA oligonucleotide along with pMiR-Reporter Vector was employed to construct reporter vectors. XIST wild type/mutant (XIST-WT/MUT) and Bax-WT/MUT were transfected into HEK293 cells with miR-150-5p-mimics and negative control (miR-NC), respectively. The cells were incubated for 24 h to detect Luciferase activity with a Dual-Luciferase reporter kit (Promega, Madison, WI, USA).

### RNA Immunoprecipitation (RIP)

RIP was conducted with an EZ-Magna RIP kit (Millipore, Billerica, MA, USA). The specific steps were as follows: H9c2 cells were lysed using radio immunoprecipitation assay (RIPA) buffer, and then the protein extract was cultured with RIP washing buffer comprising magnetic beads bound with anti-Argonaute2 (AgO2; Millipore, Billerica, MA, USA) or normal mouse immunoglobulin G (IgG). Protease K was used to digest the sample protein so as to extract immunoprecipitated RNA. QRT-PCR analyzed the purified RNA to confirm the existence of targets.

### Western Blot

The proteins were lysed with RIPA buffer (Cell Signal Technology, Inc., Danvers, MA, USA), and the concentration and quantification were determined with a bicinchoninic acid (BCA) kit (Beyotime Biotechnology, Shanghai, China). Afterwards, transferred with the proteins after electrophoresis, the polyvinylidene difluoride (PVDF) membrane (Millipore, Billerica, MA, USA) was sealed with skim milk and cultured overnight with primary antibody at 4°C. Thereafter, the membrane was incubated along with beta-actin secondary antibody for another 1 h at indoor temperature. The bands were visualized by enhanced chemiluminescence (ECL) detection system (Thermo Fisher Scientific, Waltham, MA, USA).

### Statistical Analysis

GraphPad 7 (GraphPad Inc., San Diego, CA, USA) was employed for building graphs and processing data. Inter-group comparison was conducted with independent *t*-test, and multi-group comparison with one-way analysis of variance (ANOVA) (denoted by *F*). The post-hoc comparison was conducted with Fisher's least significant difference-*t* test, the expression at multiple time points was analyzed with repeated measurement ANOVA (denoted by *F*), and the post-hoc test was carried out with Bonferroni. $p < 0.05$ was considered as statistically significant difference.

## Results

### Expression of XIST in Mice with AMI

To determine the expression of XIST in AMI mice, we established I/R models, and the modeling was examined through the cardiac function of mice and hematoxylin-eosin (HE) staining. Subsequently, it was turned out that the expression of XIST in the model group was remarkably elevated than that in the control group (Figure 1).

### XIST is Highly Expressed in Hypoxic H9c2 Cells

After hypoxia induction for 4 h, the viability, migration, and apoptosis in H9c2 cells were detected. The results showed that the viability was significantly inhibited after hypoxia induction, the invasion was slowed down, and the apoptotic rate was significantly increased. Besides, the expression of hypoxia-inducible protein (HIF-α) and apoptosis-associated proteins (Caspase-3 and Caspase-9) in H9c2 cells was also elevated after hypoxia induction. In addition, the relative expression of XIST was increased. These indicated that XIST was involved in hypoxia-induced injury in H9c2 cells (Figure 2).

### Knockdown of XIST Alleviates Hypoxia-Induced Injury in H9c2 Cells

We confirmed the over expression of XIST in H9c2 cells. To prove that XIST alleviates of H9c2 cell injury, we knocked down its expression. Hypoxia+sh-NC and Hypoxia+sh-XIST groups were established respectively. After knocking down XIST, the cell viability in Hypoxia+sh-XIST group was remarkably increased compared with Hypoxia group, the invasion was accelerated, and the apoptotic rate was reduced. Protein detection also showed that the expression of HIF-α, Caspase-3, and Caspase-9 proteins in Hypoxia+sh-XIST group was remarkably decreased compared with the Hypoxia group. These findings indicated that knocking down XIST inhibited apoptosis of H9c2 cells and improved cell viability (Figure 3).

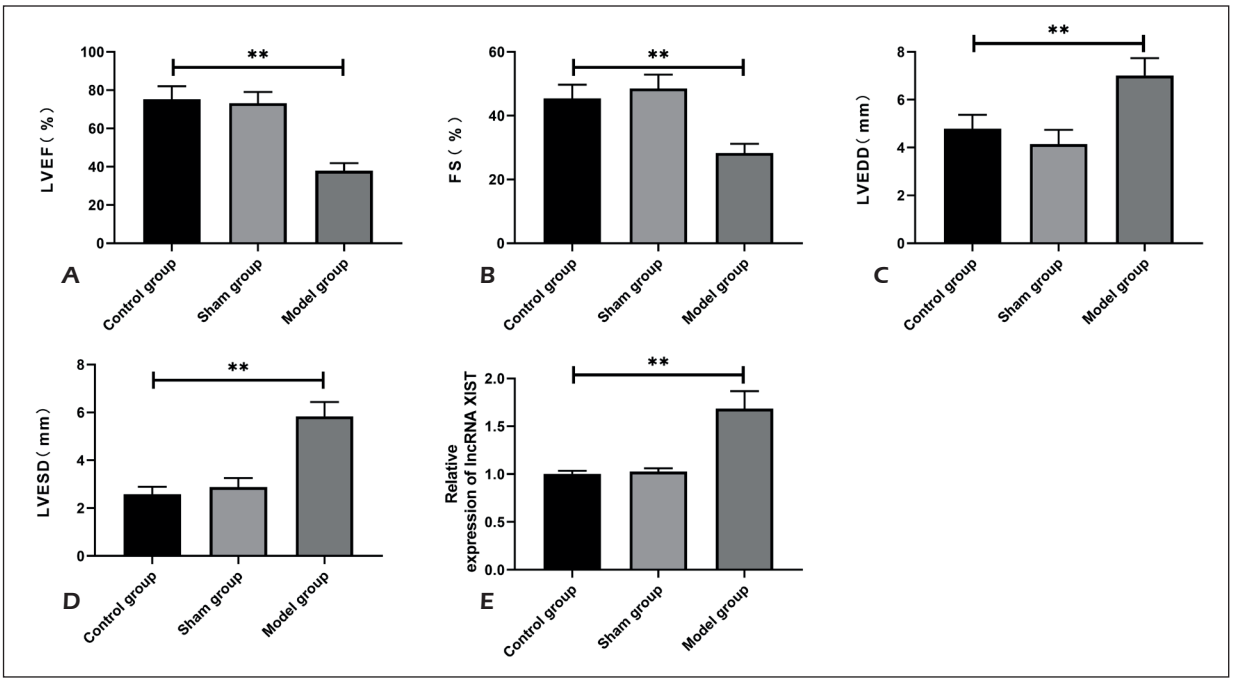


**Figure 1.** Expression of XIST in mice with AMI. ***A***, Changes of LVEF after modeling. ***B***, Changes of FS after modeling. ***C***, Changes of LVEDD after modeling. ***D***, Changes of LVESD after modeling. ***E***, Changes of XIST after modeling. LVEF: left ventricular ejection fraction; FS: fractional shorting; LVEDD: left ventricular end-diastolic diameter; LVESD: left ventricular end systolic diameter.

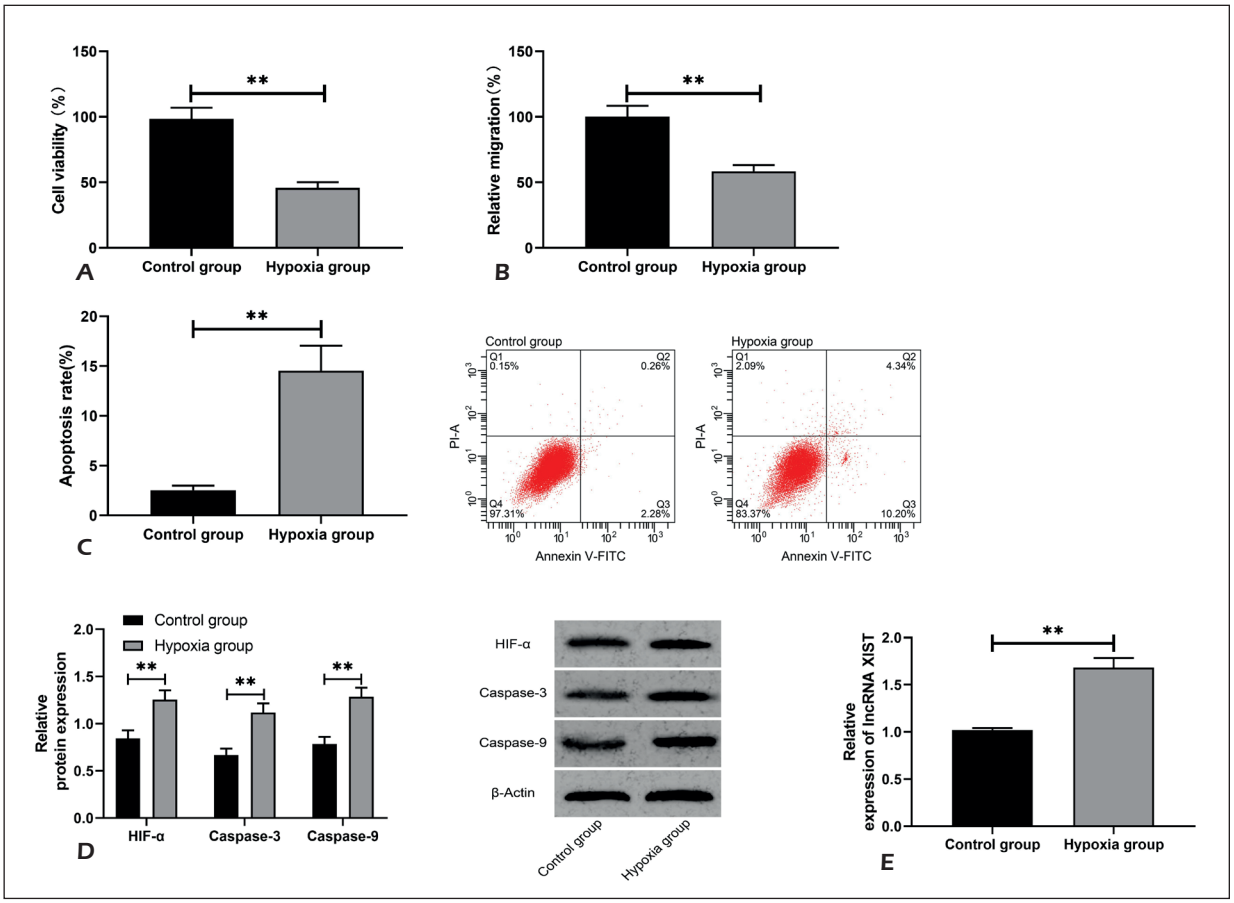


**Figure 2.** Changes of H9c2 cells and expression of XIST after hypoxia induction. ***A***, Viability of H9c2 cells after hypoxia induction. ***B***, Invasion of H9c2 cells after hypoxia induction. ***C***, Apoptotic rate of H9c2 cells after hypoxia induction. ***D***, Relative expression of HIF-α, Caspase-3, and Caspase-9 proteins in H9c2 cells after hypoxia induction. ***E***, Changes of XIST expression in H9c2 cells after hypoxia induction. ** $p<0.01$.

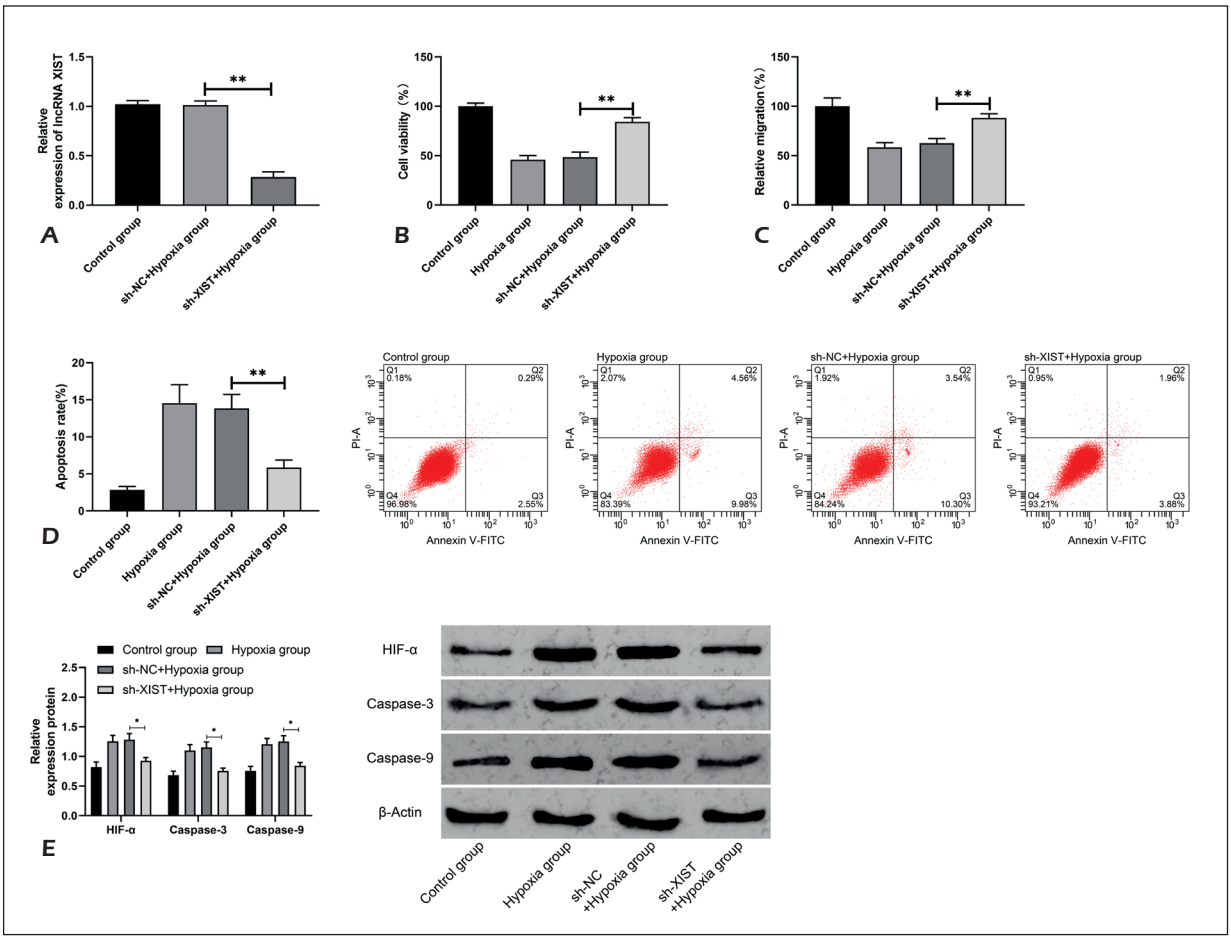


**Figure 3.** Effects of knockdown of XIST on H9c2 cells. **A**, Changes of relative expression of XIST in H9c2 cells after sh-XIST transfection. **B**, Influences of sh-XIST transfection on viability. **C**, Influences of sh-XIST transfection on invasion. **D**, Influences of sh-XIST transfection on apoptosis. **E**, Influences of sh-XIST transfection on expression of HIF-α, Caspase-3, and Caspase-9 proteins. *$p<0.05$, **$p<0.01$.

### *XIST Serves as A MiR-150-5p Sponge*

Through StarBase 3.0, we noticed that XIST shared targeted binding sites with miR-150-5p. Then, we performed RIP and Dual-Luciferase reporter assay to exhibit the association between the two. RIP illustrated that both miR-150-5p and XIST could be precipitated by Ago2 and neither could be precipitated by IgG. Dual-Luciferase reporter assay demonstrated that the fluorescence activity of XIST-WT was suppressed by miR-150-5p-mimics and enhanced by miR-150-5p-inhibit. Moreover, it found out that miR-150-5p was elevated in cells transfected with sh-XIST. These results confirmed that XIST functioned as a miR-150-5p sponge to produce regulatory effect (Figure 4).

### *Up-regulation of MiR-150-5p Inhibits Bax and Reduces Apoptosis of H9c2 Cells*

To explore the mechanism of miR-150-5p, we predicted its downstream target genes using Starbase 3.0 and found that Bax shared targeted binding sites with miR-150-5p, which was confirmed by Dual-luciferase reporter assay. The relative expression of Bax protein and mRNA in H9c2 cells was significantly inhibited after miR-150-5p was up-regulated, while the results were reversed after miR-150-5p was knocked down. To further determine the relationship between the two, miR-NC+-si-NC, pcDNA3.1-Bax, miR-150-5pmimics, and pcDNA3.1-Bax+miR-150-5p-mimics were transfected into H9c2 cells for hypoxia induction. The cell viability, invasion, as well as apoptosis were

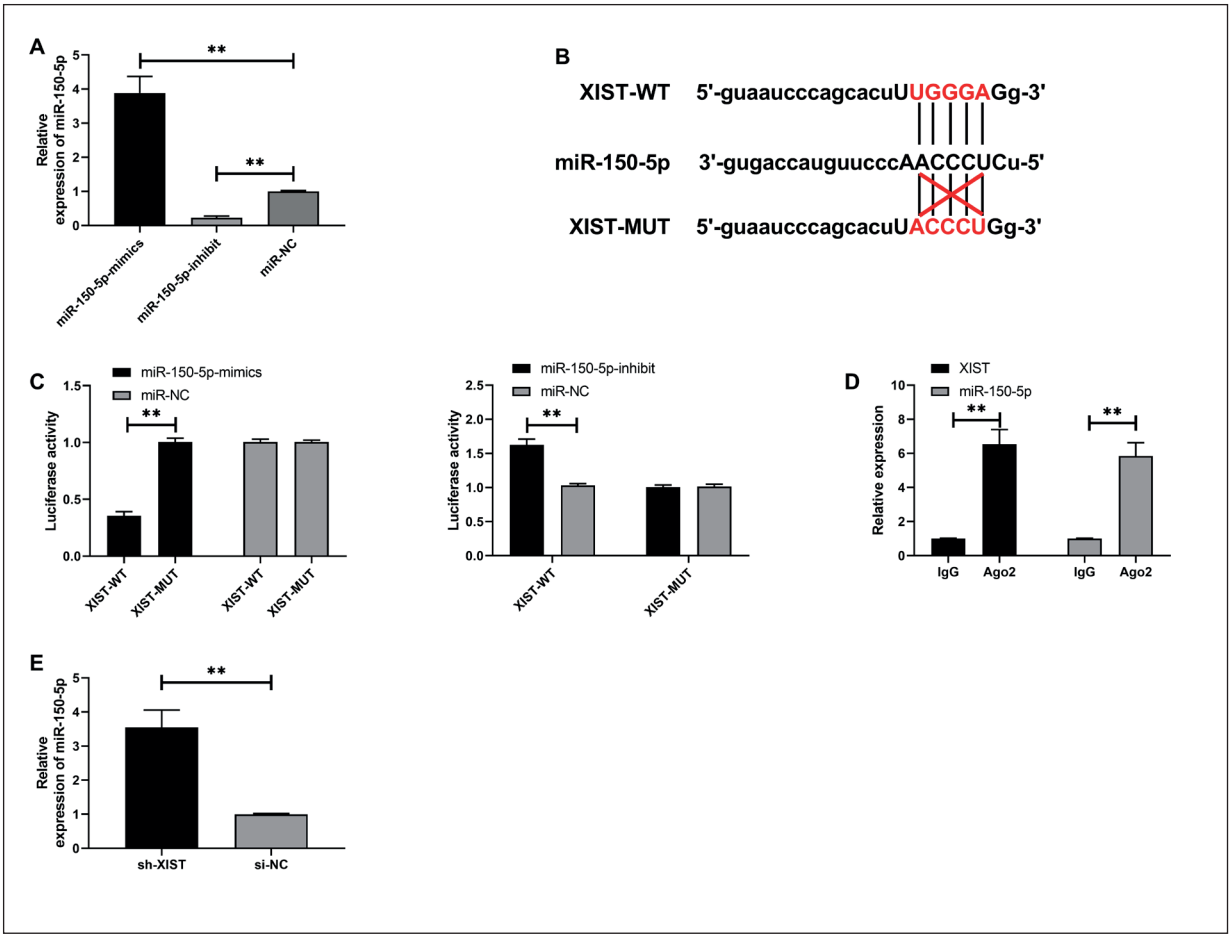


**Figure 4.** XIST shares targeted binding sites with miR-150-5p. **A**, Expression of miR-150-5p in cells transfected with miR-150-5p inhibit or mimics. **B**, Binding sites between XIST and miR-150-5p. **C**, Dual-Luciferase reporter assay indicates the targeting relation between miR-150-5p and XIST. **D**, RIP shows that XIST and miR-150-5p can be precipitated by Ago2. **E**, Relative expression of miR-150-5p in cells transfected with sh-XIST.

detected. The apoptosis of cells transfected with pcDNA3.1-Bax was significantly accelerated, and the viability and invasion were weakened. However, the results were reversed after co-transfection of miR-150-5pmimics and pcDNA3.1-Bax. Western blot indicated that Bax, Caspase-3, and Caspase-9 proteins decreased and the Bcl-2 increased after up-regulating miR-150-5p, but the outcome was reversed after co-transfection, suggesting that miR-150-5p targeted Bax to regulate cell apoptosis, thus affecting cell viability and invasion (Figure 5).

### *XIST Inhibits Apoptosis of H9c2 Cells by Mediating MiR-150-5p/Bax Axis*

We established sh-XIST+miR-150-5p-inhibit, sh-XIST+pcDNA3.1-Bax to verify that XIST can protect cardiomyocytes via the miR-150-5p/Bax axis. Cell viability and invasion were enhanced, and the apoptosis was decreased after knockdown of XIST. However, the results were reversed after co-transfection with miR-150-5p-inhibit or pcDNA3.1-Bax. Western blot also revealed that Bax, Caspase-3, and Caspase-9 proteins in H9c2 cells were down-regulated and Bcl-2 was up-regulated and the results were reversed after co-transfection (Figure 6).

## Discussion

Hypoxia-induced cardiomyocyte injury contributes to AMI, heart failure, and other CVDs[20,21]. Despite the great advancements in medical technology and the improvement of prognosis of patients, CVDs still have the highest mortality and prevalence in the world[22,23]. Therefore, exploring the mechanism of hypoxia-induced cardiomyocyte injury is a top priority.

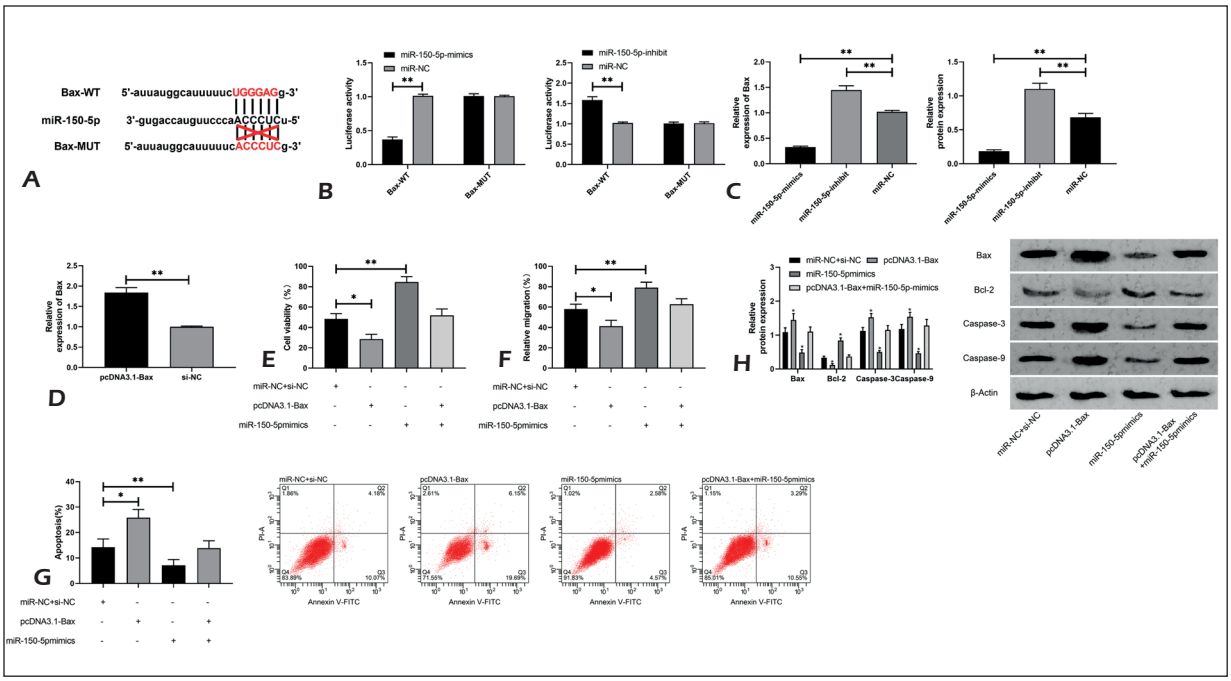


**Figure 5.** MiR-150-5p targets Bax to inhibit apoptosis of H9c2 cells. **A**, Targeted binding sites between Bax and miR-150-5p. B, Dual-Luciferase reporter assay confirms the targeting relation between Bax and miR-150-5p. **C**, MRNA and protein expression in H9c2 cells transfected with miR-150-5p inhibit or mimics. **D**, Relative expression of Bax in cells transfected with pcDNA3.1-Bax. **E**, Changes of cell viability after transfection. **F**, Changes of invasion after transfection. **G**, Changes of apoptosis after transfection. **H**, Changes of protein expression after transfection.

LncRNAs are involved in the progression of tumors, CVDs, and neurological diseases[24-26]. XIST, the first class of lncRNA discovered, is highly expressed in gastric cancer[27] and myocardial anoxia/reperfusion injury[17]. However, the relevant mechanism remains unknown. In this study, the expression of XIST was remarkably elevated in hypoxic H9c2 cells, cell viability and invasion

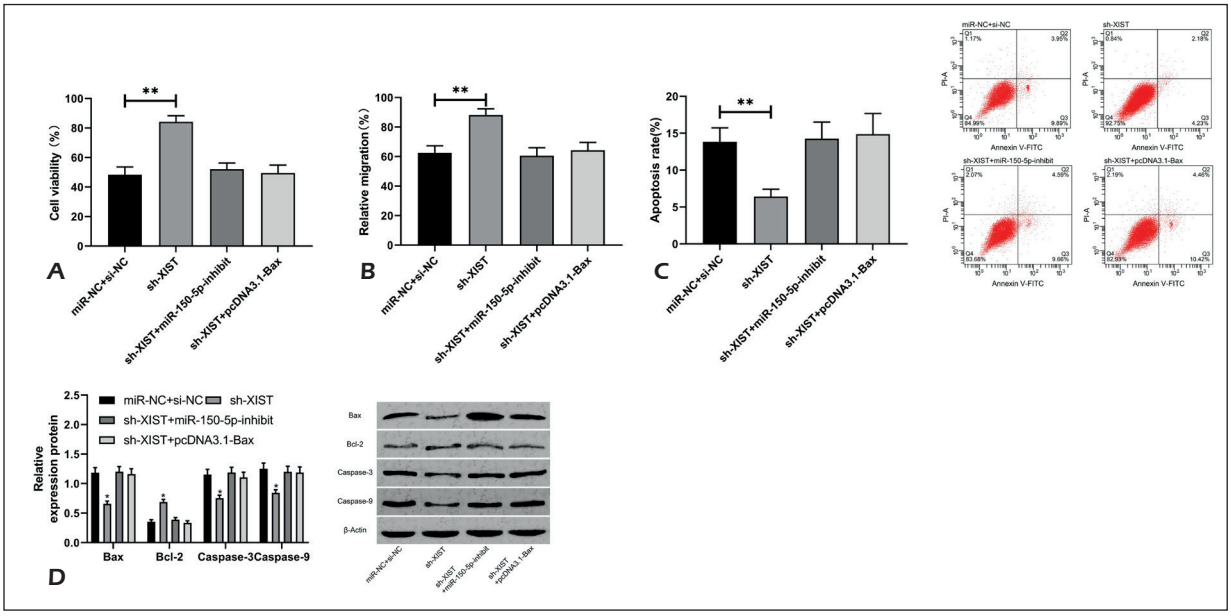


**Figure 6.** XIST enhances the viability of H9c2 cells by mediating miR-150-5p/Bax-axis. **A**, Changes of cell viability after co-transfection. **B**, Changes of cell invasion after co-transfection. **C**, Changes of apoptosis after co-transfection. **D**, Changes of protein expression after co-transfection

were significantly enhanced, and the apoptosis was reduced after knocking down XIST, which indicated that XIST was a potential target for the treatment of CVDs. Therefore, we explored the related mechanism.

MiRs, a hot topic in various disciplines, are a kind of small non-coding RNAs (~21-25 nucleotides) participating in cell regulation, energy metabolism, apoptosis, and other processes. Moreover, they degrade mRNA or suppress protein translation in the way of binding to the 3' untranslated region (3'UTR) of target genes[28-30]. In addition, several miRs exhibit differential expression during the development of AMI[31,32]. LncRNA regulates miR expression by acting as a ceRNA to compete with miR for MREs[33,34]. Therefore, we predicted candidate miRs that XIST can bind to, and noticed that there were binding sites between XIST and miR-150-5p. MiR-150-5p is located on human 19q13.33 chromosome, and its low expression is a risk factor for mortality within 90 days after acute ischemic stroke[35]. It can delay myocardial fibrosis via targeting early growth response 1 (EGR1)[36]. In this research, RIP and Dual-Luciferase reporter assay were conducted to figure out the correlation of XIST with miR-150-5p. We acquired that miR-150-5p and XIST were precipitated by Ago2. In addition, Dual-Luciferase reporter assay demonstrated that the fluorescence activity of XIST-WT was regulated by miR-150-5p-mimics/inhibit, which suggested that XIST inhibited hypoxia-induced cardiomyocyte apoptosis by regulating miR-150-5p.

Target gene prediction was conducted to investigate the related mechanism of miR-150-5p and indicated that Bax was a potential target gene of miR-150-5p. The relationship between the two was verified by the Dual-Luciferase reporter assay. Bax is the most important apoptosis gene in human body belonging to Bcl-2 gene family[37]. In our study, the apoptosis of cells transfected with pcDNA3.1-Bax was significantly accelerated, and the viability and invasion were reduced. However, the results were reversed after co-transfection of miR-150-5pmimics and pcDNA3.1-Bax, suggesting that XIST was involved in hypoxia-induced injury by mediating miR-150-5p/Bax axis. At the end of the study, sh-XIST+miR-150-5p-inhibit and sh-XIST+pcDNA3.1-Bax were constructed in order to verify that XIST was able to protect the cells from hypoxia-induced injury by mediating miR-150-5p/Bax. After knocking down XIST, cell viability and invasion was enhanced, and the apoptosis was decreased. Co-transfection with miR-150-5P-inhibit and pcDNA3.1-Bax reversed the outcome.

Through the above tests, we basically confirm that XIST participates in hypoxia-induced injury by mediating miR-150-5p/Bax axis. However, there are several limitations. First, we have not detected the expression of XIST in patients. Then, we have not established animal models and only explored the relevant mechanism of XIST through cell model. Therefore, we will carry out more clinical trials and animal researches to verify our conclusions.

## Conclusions

In sum, XIST protects cardiomyocytes from hypoxia-induced injury by mediating miR-150-5p/Bax axis, suggesting that XIST is an important target for AMI treatment.

### Acknowledgments

This research received no specific grant from any funding agency in the public, commercial, or not-for-profit sectors.

### Conflict of Interests

The authors declare that they have no conflict of interests.

## References

1) Semenciw RM, Morrison HI, Mao Y, Johansen H, Davies JW, Wigle DT. Major risk factors for cardiovascular disease mortality in adults: results from the Nutrition Canada Survey cohort. Int J Epidemiol 1988; 17: 317-324.
2) Go AS, Mozaffarian D, Roger VL, Benjamin EJ, Berry JD, Borden WB, Bravata DM, Dai S, Ford ES, Fox CS, Franco S, Fullerton HJ, Gillespie C, Hailpern SM, Heit JA, Howard VJ, Huffman MD, Kissela BM, Kittner SJ, Lackland DT, Lichtman JH, Lisabeth LD, Magid D, Marcus GM, Marelli A, Matchar DB, McGuire DK, Mohler ER, Moy CS, Mussolino ME, Nichol G, Paynter NP, Schreiner PJ, Sorlie PD, Stein J, Turan TN, Virani SS, Wong ND, Woo D, Turner MB; American Heart Association Statistics Committee and Stroke Statistics Subcommittee. Heart disease and stroke statistics--2013 update: a report from the American Heart Association. Circulation 2013; 127: e6-e245.
3) Bajaj A, Sethi A, Rathor P, Suppogu N, Sethi A. Acute complications of myocardial infarction in the current era: diagnosis and management. J Investig Med 2015; 63: 844-855.
4) Holmes DR Jr. Cardiogenic shock: a lethal complication of acute myocardial infarction. Rev Cardiovasc Med 2003; 4: 131-135.

5) Cheng WP, Lo HM, Wang BW, Chua SK, Lu MJ, Shyu KG. Atorvastatin alleviates cardiomyocyte apoptosis by suppressing TRB3 induced by acute myocardial infarction and hypoxia. J Formos Med Assoc 2017; 116: 388-397.
6) Zhang Y, Shen T, Liu B, Dai D, Cai J, Zhao C, Du L, Jia N, He Q. Cardiac shock wave therapy attenuates cardiomyocyte apoptosis after acute myocardial infarction in rats. Cell Physiol Biochem 2018; 49: 1734-1746.
7) Vausort M, Wagner DR, Devaux Y. Long noncoding RNAs in patients with acute myocardial infarction. Circ Res 2014; 115: 668-677.
8) Weidle UH, Birzele F, Kollmorgen G, Ruger R. Long non-coding RNAs and their role in metastasis. Cancer Genomics Proteomics 2017; 14: 143-160.
9) Bhan A, Soleimani M, Mandal SS. Long noncoding RNA and cancer: a new paradigm. Cancer Res 2017; 77: 3965-3981.
10) Zhang X, Hamblin MH, Yin KJ. The long noncoding RNA Malat1: its physiological and pathophysiological functions. RNA Biol 2017; 14: 1705-1714.
11) Zhuo LA, Wen YT, Wang Y, Liang ZF, Wu G, Nong MD, Miao L. LncRNA SNHG8 is identified as a key regulator of acute myocardial infarction by RNA-seq analysis. Lipids Health Dis 2019; 18: 201.
12) Yang J, Huang X, Hu F, Fu X, Jiang Z, Chen K. LncRNA ANRIL knockdown relieves myocardial cell apoptosis in acute myocardial infarction by regulating IL-33/ST2. Cell Cycle 2019; 18: 3393-3403.
13) Engreitz JM, Pandya-Jones A, McDonel P, Shishkin A, Sirokman K, Surka C, Kadri S, Xing J, Goren A, Lander ES, Plath K, Guttman M. The Xist lncRNA exploits three-dimensional genome architecture to spread across the X chromosome. Science 2013; 341: 1237973.
14) Chen DL, Ju HQ, Lu YX, Chen LZ, Zeng ZL, Zhang DS, Luo HY, Wang F, Qiu MZ, Wang DS, Xu DZ, Zhou ZW, Pelicano H, Huang P, Xie D, Wang FH, Li YH, Xu RH. Long non-coding RNA XIST regulates gastric cancer progression by acting as a molecular sponge of miR-101 to modulate EZH2 expression. J Exp Clin Cancer Res 2016; 35: 142.
15) Kong Q, Zhang S, Liang C, Zhang Y, Kong Q, Chen S, Qin J, Jin Y. LncRNA XIST functions as a molecular sponge of miR-194-5p to regulate MAPK1 expression in hepatocellular carcinoma cell. J Cell Biochem 2018; 119: 4458-4468.
16) Tang Y, He R, An J, Deng P, Huang L, Yang W. LncRNA XIST interacts with miR-140 to modulate lung cancer growth by targeting iASPP. Oncol Rep 2017; 38: 941-948.
17) Zhang M, Liu HY, Han YL, Wang L, Zhai DD, Ma T, Zhang MJ, Liang CZ, Shen Y. Silence of lncRNA XIST represses myocardial cell apoptosis in rats with acute myocardial infarction through regulating miR-449. Eur Rev Med Pharmacol Sci 2019; 23: 8566-8572.
18) Liu H, Xu D, Zhong X, Xu D, Chen G, Ge J, Li H. LncRNA-mRNA competing endogenous RNA network depicts transcriptional regulation in ischaemia reperfusion injury. J Cell Mol Med 2019; 23: 2272-2276.
19) Livak KJ, Schmittgen TD. Analysis of relative gene expression data using real-time quantitative PCR and the 2(-Delta Delta C(T)) method. Methods 2001; 25: 402-408.
20) Ashley Z, Schwenke DO, Cragg PA. Hyperventilation in normoxia following myocardial infarction in rats: a shift in the set point of the hypoxic ventilatory response. Acta Physiol (Oxf) 2015; 214: 415-425.
21) Lim GB. Acute coronary syndromes: Supplemental oxygen in myocardial infarction. Nat Rev Cardiol 2017; 14: 632.
22) Nishino S, Watanabe N, Kimura T, Enriquez-Sarano M, Nakama T, Furugen M, Koiwaya H, Ashikaga K, Kuriyama N, Shibata Y. The course of ischemic mitral regurgitation in acute myocardial infarction after primary percutaneous coronary intervention: from emergency room to long-term follow-up. Circ Cardiovasc Imaging 2016; 9: e004841.
23) Nuding S, Werdan K, Prondzinsky R. Optimal course of treatment in acute cardiogenic shock complicating myocardial infarction. Expert Rev Cardiovasc Ther 2018; 16: 99-112.
24) Andersen RE, Lim DA. Forging our understanding of lncRNAs in the brain. Cell Tissue Res 2018; 371: 55-71.
25) Uchida S, Dimmeler S. Long noncoding RNAs in cardiovascular diseases. Circ Res 2015; 116: 737-750.
26) Viereck J, Thum T. Circulating noncoding RNAs as biomarkers of cardiovascular disease and injury. Circ Res 2017; 120: 381-399.
27) Li Y, Zhang Q, Tang X. Long non-coding RNA XIST contributes into drug resistance of gastric cancer cell. Minerva Med 2019; 110: 270-272.
28) Fan W, Liu Y, Li C, Qu X, Zheng G, Zhang Q, Pan Z, Wang Y, Rong J. MicroRNA-331-3p maintains the contractile type of vascular smooth muscle cells by regulating TNF-alpha and CD14 in intracranial aneurysm. Neuropharmacology 2019 Nov 27:107858. doi: 10.1016/j.neuropharm.2019.107858. [Epub ahead of print]
29) Jin Z, Ren J, Qi S. Human bone mesenchymal stem cells-derived exosomes overexpressing microRNA-26a-5p alleviate osteoarthritis via down-regulation of PTGS2. Int Immunopharmacol 2020; 78: 105946.
30) Yao HL, Liu M, Wang WJ, Wang XL, Song J, Song QQ, Han J. Construction of miRNA-target networks using microRNA profiles of CVB3-infected HeLa cells. Sci Rep 2019; 9: 17876.
31) Gao C, Zhao D, Wang J, Liu P, Xu B. Clinical significance and correlation of microRNA-21 expression and the neutrophil-lymphocyte ratio in patients with acute myocardial infarction. Clinics (Sao Paulo) 2019; 74: e1237.
32) Tian HB, Li SH, Hu KQ, Zan YS, Zhang XL, Su GH. MicroRNA-150 alleviates acute myocardial infarction through regulating cardiac fibroblasts in ventricular remodeling. Eur Rev Med Pharmacol Sci 2019; 23: 7611-7618.
33) Qi X, Zhang DH, Wu N, Xiao JH, Wang X, Ma W. CeRNA in cancer: possible functions and clinical implications. J Med Genet 2015; 52: 710-718.

34) Xu J, Li Y, Lu J, Pan T, Ding N, Wang Z, Shao T, Zhang J, Wang L, Li X. The mRNA related ceRNA-ceRNA landscape and significance across 20 major cancer types. Nucleic Acids Res 2015; 43: 8169-8182.
35) Scherrer N, Fays F, Mueller B, Luft A, Fluri F, Christ-Crain M, Devaux Y, Katan M. MicroRNA 150-5p improves risk classification for mortality within 90 days after acute ischemic stroke. J Stroke 2017; 19: 323-332.
36) Shen J, Xing W, Gong F, Wang W, Yan Y, Zhang Y, Xie C, Fu S. MiR-150-5p retards the progression of myocardial fibrosis by targeting EGR1. Cell Cycle 2019; 18: 1335-1348.
37) Song ZC, Chen L, Zhang D, Zhang SY, Lin X. Rosuvastatin protects acute myocardial infarction rats through autophagy regulation via AMPK signaling. Zhonghua Yi Xue Za Zhi 2018; 98: 3536-3541.